# Kernel-Phase Interferometry for Super-Resolution Detection of Faint Companions

TEXAS
The University of Texas at Austin

**Samuel M. Factor**, Adam L. Kraus
Dept. of Astronomy, The University of Texas at Austin

**Contact Information**
Website: smfactor.github.io
Email: sfactor@utexas.edu

S. Factor is P.I. of HST Cycle 24 Archival project 14561 which is supporting this work.

**Kernel-phases are** self-calibrating observables **used for high-contrast imaging at or even below λ/D.** We are currently using this technique to search for companions to nearby brown dwarfs in archival *HST* images. The pipeline will be particularly **applicable to JWST** and the future 30m class telescopes and will be **available soon as a python package**.

## Background

- While direct-imaging surveys are more sensitive to companions at large semimajor axes than transit and RV surveys, **there is often a gap in sensitivity between direct imaging and transit/RV surveys.**
- "Speckles," caused by imperfections in the optical path (including AO), can be corrected **but most techniques tend to fail near λ/D.**
- Interferometric analysis takes advantage of the wave nature of light and can reject speckle noise to detect companions with high contrast *at or even below* the diffraction limit. **Rather than subtracting off the PSF, interferometric techniques use the information contained in it to infer the geometry of the source.** The discovery of the proposed newly forming giant planet LkCa15 b by Kraus & Ireland (2012) demonstrates the power of such techniques.

**Filling the gap between transit/RV surveys and classical direct-imaging surveys would offer a crucial new view of both exoplanetary systems and stellar multiplicity.**

## What is a Kernel-Phase?

Non-redundant aperture masking interferometry (NRM or AMI) places a mask in the pupil plane, transforming a large single aperture into a sparse interferometer. This mask blocks ~95% of the gathered light, imposing a *severe* flux limit. **Kernel-phase analysis models the *full aperture* as a grid of sub-apertures** (Fig. 1). This model defines which spatial frequencies are sampled. We then examine the *phase* of the Fourier transform of the images to infer the source geometry.

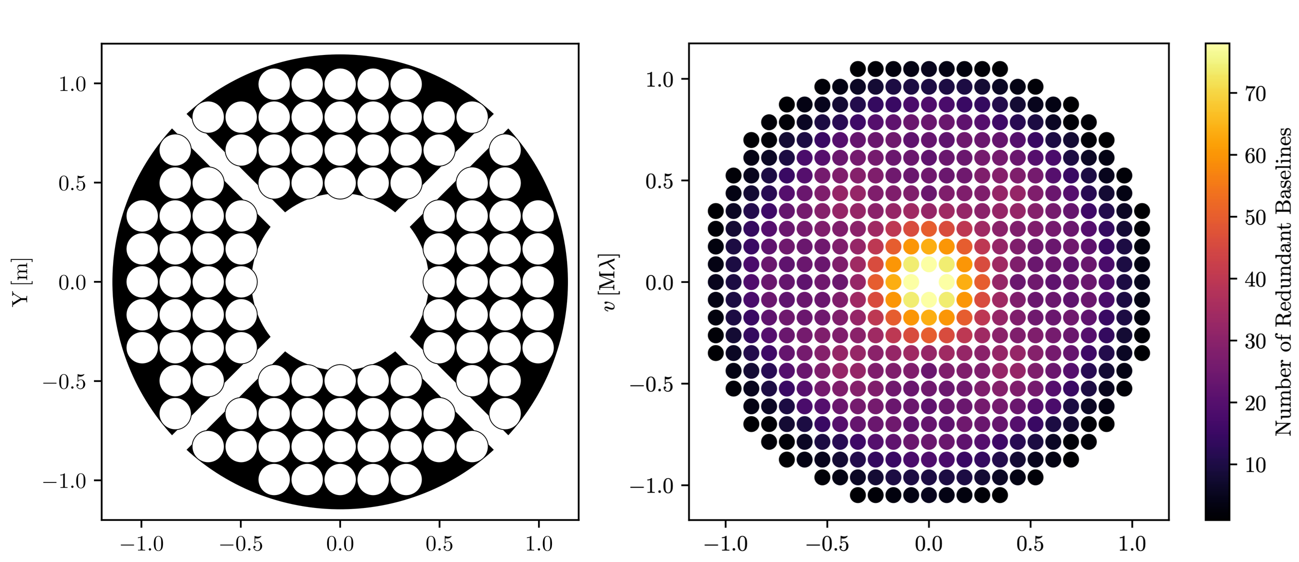

Figure 1: *Left*: HST aperture (black) and simulated sub-apertures (white circles). *Right*: The matching baselines (at 1.7 μm), color coded by their redundancy. The 104 simulated sub-apertures sample 258 unique baselines and generate 206 kernel-phases.

Each pair of apertures, or baseline, contributes both the true phase of the source and a phase error from each of the apertures. Combining all the baselines, we can write a matrix equation for the measured phases:

$$\Phi = \Phi_\circ + \mathbf{A} \cdot \phi \qquad (1)$$

Where Φ a vector of the measured phases from each baseline, $\Phi_0$ is the true source phase, **A** is a matrix encoding which apertures contribute to each baseline, and ϕ is the phase errors of each aperture. Columns and rows of **A** correspond to apertures and baselines, respectively.

To derive an equation independent of the phase errors, we calculate the kernel (**K**) of **A**:

$$\mathbf{K} \cdot \mathbf{A} = 0 \qquad (2)$$

We can then multiply both sides of Equation 1 by **K** to get

$$\mathbf{K} \cdot \Phi = \mathbf{K} \cdot \Phi_\circ + \mathbf{K} \cdot \mathbf{A} \cdot \phi$$
$$= \mathbf{K} \cdot \Phi_\circ \qquad (3)$$

This produces observables called kernel-phases (first presented by Martinache 2010) which are independent of phase errors, similar to closure-phases used with NRM. **This technique can achieve similar detection limits to NRM in a fraction of the time and can be applied to dimmer sources where NRM is not feasible, as well as archival data sets.**

## From Image to Kernel-Phase to Fitting

We are currently analyzing a large set of NICMOS1 observations to search for compact binary brown dwarf systems. **We use Bayesian model comparison** (using `PyMultiNest`; Buchner et al. 2014) **to compare one and two point-source models**. Fig. 2 & 3 show analysis of images from Reid et al. (2006).

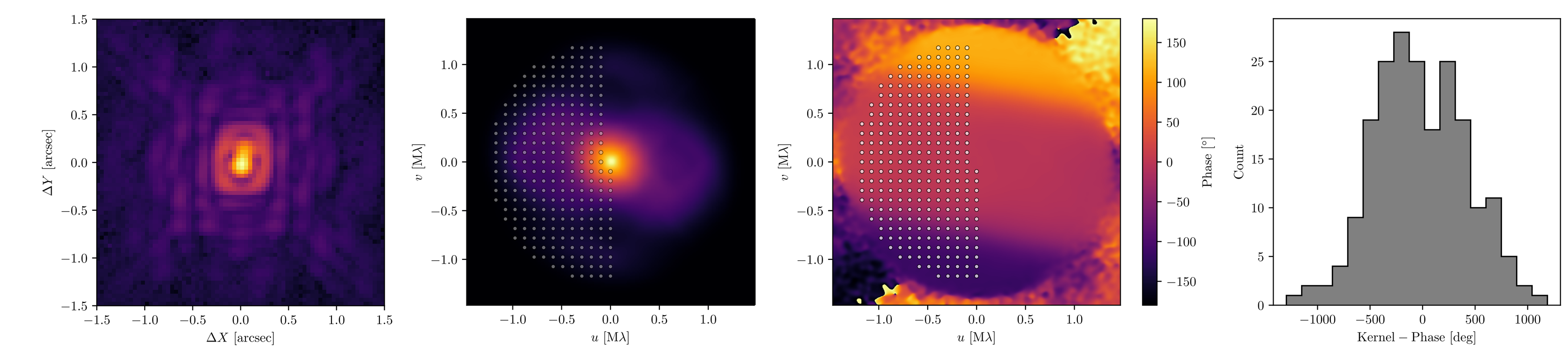

Figure 2: The progression from image to kernel-phase for an observation of 2MASS J0147-4954, a brown dwarf with a companion at ~140 mas (~1 λ/D) and ~2:1 contrast in F170M. *From left to right*: NICMOS1 image (fourth root scaling), Fourier-amplitude, Fourier-phase (grey circles show the model baselines from Fig. 2), and resulting kernel-phases. Science target kernel-phases must then be calibrated by subtracting the kernel-phases from a singular source.

Figure 3: Results of fitting a double point-source model to observations of 2MASS J2351-2537 (example image shown in the upper right corner). *Lower Left*: Corner plot showing the posteriors of the four-parameter fit. *Top Right*: Data kernel-phases plotted against the best-fit model kernel-phases indicating a good fit. Detection limits for this fit show it is significant at the 5σ level, while the Bayes-factor shows "decisive evidence" of a binary.

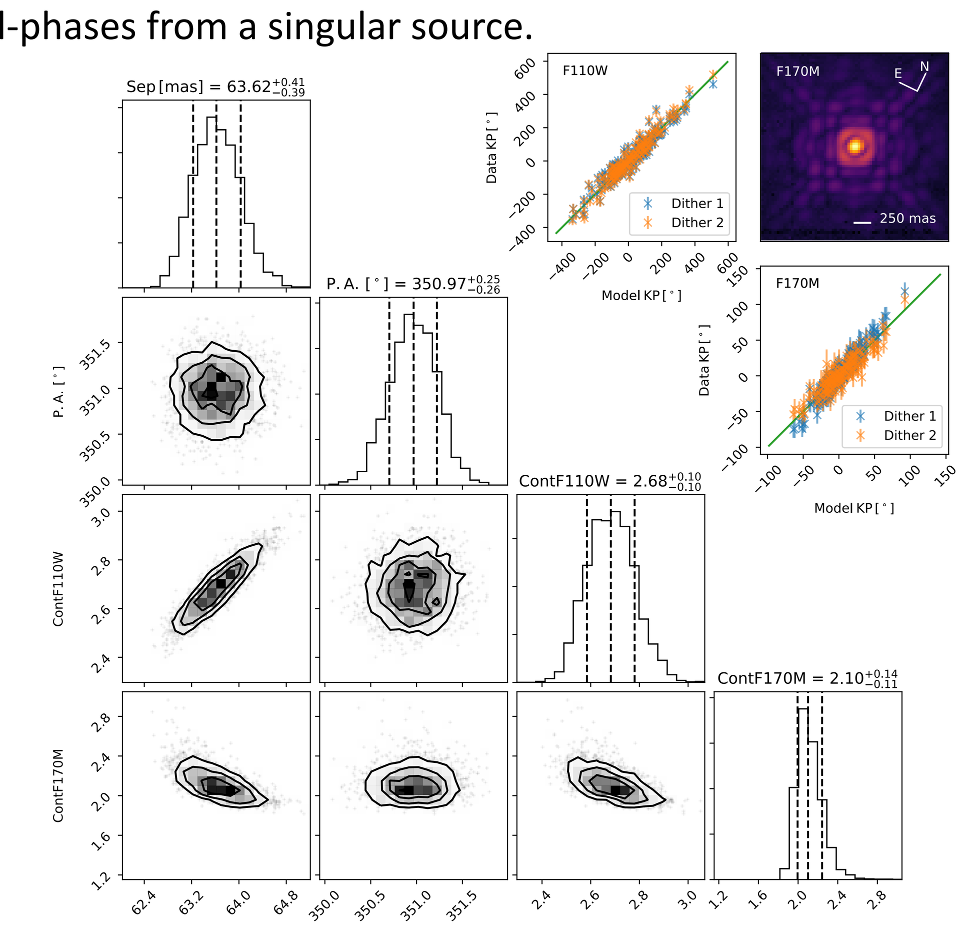

## Results: A widely applicable pipeline for high contrast imaging at λ/D

Previous estimates of the detection limits (Martinache 2010, Pope et al. 2013) show a detection with **~50:1 contrast at 80 mas (0.5λ/d at 1.9 μm) or ~3:1 contrast at 35 mas** is possible with 99% confidence. In star-forming regions like Taurus (~1-5 Myr, ~140 pc), this corresponds to a few $M_{Jup}$ mass planet at 10 au around a late M/brown dwarf or a similar mass binary at 5 au.

The stacked 5σ detection limits for our sample along with detections and notable non-detections are shown in Fig. 4.

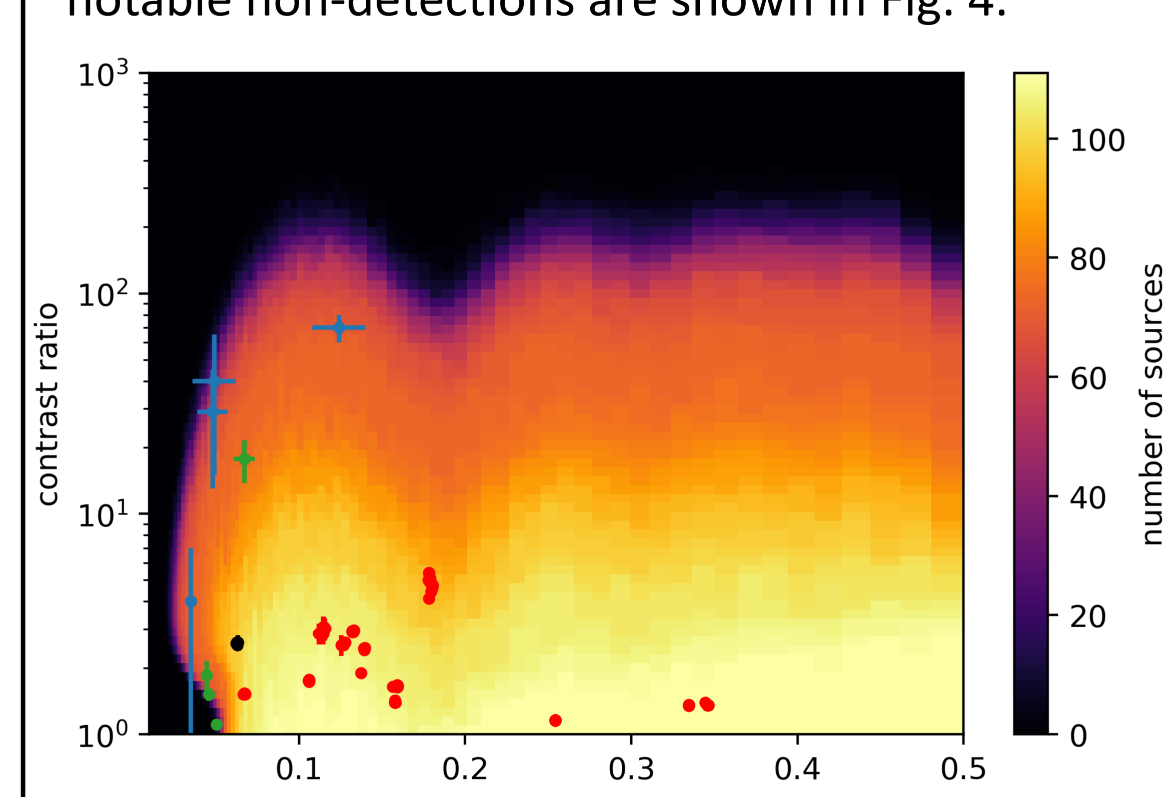


Figure 4: Stacked 5σ detection limits for all sources in our sample calculated using a method similar to NRM. New realizations of the noise are created by scrambling the (best-fit) model subtracted kernel-phases. We then fit the contrast on a grid in separation and PA. The 99% confidence contrast is then the level at which 99% of all fits are fainter. Red points show detected companions, green (blue) points are new (marginal) detections from Pope et al. (2013) which we *do not significantly detect*. The black point is the one detection from Pope et al. (2013) that we confirm (2MASS J2351-2537, shown above and below).

Figure 5: 99% sensitivity in F170M as a function of separation and PA around the single source used in Fig. 4 (*left*, detector PA) and the binary 2MASS J2351-2537 (*right*, sky PA) after subtracting the best fit model shown in Fig. 3. The position of the companion is indicated by the white dot.